

## EMPIRICALLY OPTIMUM M1 OPERATOR FOR sd-SHELL NUCLEI

B.A. BROWN

*Cyclotron Laboratory and Department of Physics and Astronomy, Michigan State University,  
East Lansing, MI 48824, USA*

B.H. WILDENTHAL

*Physics Department, Drexel University, Philadelphia, PA 19104, USA\**

Received 11 May 1987

**Abstract:** M1 matrix elements deduced from experimental data on M1 transitions and magnetic moments in the sd-shell nuclei are analysed with calculations based on the full-basis sd-shell wave functions of Wildenthal to extract the parameters for an effective M1 operator. These empirical parameters are analogous to the predicted corrections for the free-nucleon M1 operator which arise from the effects of higher-order configuration mixing and mesonic-exchange currents. From the differences between the effective operators associated with isoscalar M1 matrix elements, isovector M1 matrix elements, and Gamow-Teller (GT) matrix elements (as deduced previously from GT beta decay data) we are able to evaluate the relative importance of higher-order configuration mixing, mesonic exchange currents involving the  $\Delta$ -isobar, and other mesonic exchange currents.

### 1. Introduction

Magnetic moments, M1 gamma decay, and Gamow-Teller beta decay provide clear and direct information about nuclear structure because of the simple forms of the associated operators. In particular, study of these phenomena can yield information about the natures of the electromagnetic and weak interactions in nuclei and about the multiparticle structure of nuclear wave functions. This paper presents results of an empirical determination of the optimum form of the M1 operator in nuclei, as obtained from an analysis of experimental data for  $A = 17-39$  nuclei in the context of large-basis  $0d_{5/2}-1s_{1/2}-0d_{3/2}$  (sd) shell-model calculations.

The standard or "free-nucleon" form of the M1 operator incorporates the measured properties of the free proton and neutron as the coefficients of the intrinsic spin and orbital operators. The single-particle matrix elements of this free-nucleon operator can be combined with the one-body densities calculated from the multiparticle shell-model wave functions to give "free-nucleon" values of the M1 matrix elements. Renormalizations, or higher-order corrections, for the standard-form operator can be extracted by finding the adjustments of the single-particle matrix elements which minimize the deviations between the "free-nucleon" multiparticle

\* Present address: Department of Physics and Astronomy, University of New Mexico, Albuquerque, NM 87131, USA.

M1 matrix elements and experimental values. The goal is to better understand the details of specific observed M1 phenomena and the general corrections to shell-model calculations which arise from configuration mixing over many major oscillator shells, mesonic-exchange currents, isobar excitation and other higher-order effects.

We have previously determined an empirical M1 operator from a similar analysis of the magnetic moments of mirror levels in the sd-shell<sup>1)</sup>. The data set consisting only of mirror levels was chosen so as to isolate the isoscalar terms of the operator. When both isoscalar and isovector contributions are present in a single matrix element the dominance of the isovector component of the M1 operator over the isoscalar component, which arises from the opposite signs and nearly equal magnitudes of the neutron and proton magnetic moments, precludes any quantitative view of the isoscalar contributions. However, the limited number of examples in the mirror-level data set might not provide the best possible determination of the isovector operator. In the present work we incorporate all of the measured magnetic dipole moments, together with a large number of matrix elements obtained from M1 transitions, into our determination of the empirical operator.

The renormalizations of the M1 operator which we determine in this study are analogous to theoretical estimates of corrections for the effects of higher-order features of nuclear structure which are excluded from the conventional, one-major-shell, shell-model calculations<sup>2,3)</sup>. The details of these higher-order corrections have been of particular interest in the context of the apparent quenching of  $\sigma\tau$  strength in Gamow-Teller beta decay<sup>4)</sup> and analogous (p n) and (n, p) reaction cross sections<sup>5)</sup>. Theoretical studies of the renormalization effects which we study here empirically are made in the context of single-particle systems, the specific sd-shell examples of which are  $^{17}\text{O}$ - $^{17}\text{F}$  and  $^{39}\text{K}$ - $^{39}\text{Ca}$ . However, the relationships between simple single-particle models and the actual situations in  $A=17$  and  $A=39$  are somewhat ambiguous. The actual wave functions for these nuclei may have the single-particle components fragmented by admixtures with the four-particle four-hole excitations of the core. In addition, many of the transitions between the sd-shell states in  $A=17$  and  $A=39$  are unmeasurable.

From the wealth of experimental data for the nuclei in the region  $A=18-38$  it is possible, with the predicted one-body densities of the multiparticle shell-model wave functions, to extract the complete set of effective single-particle M1 matrix elements which ideally would be available from the  $A=17$  and  $A=39$  systems alone. In addition to providing a more complete characterization of the M1 operator, the results from the analysis of the multiparticle systems can buttress the unique single-particle data with many confirming data from other nuclei. With this large redundancy, specific discrepancies between experimental and model wave functions should be averaged out.

In sect. 2 the sd-shell wave functions are discussed and the formulations for the free-nucleon and effective M1 operators are given. In sect. 3 the experimental data set is defined and the comparison between theory and experiment is presented. The

effective operators deduced from this comparison, together with those obtained in previous similar comparisons for isoscalar moments and GT beta decay, are discussed in sect. 4.

## 2. Elements of the analysis

### 2.1. SHELL-MODEL WAVE FUNCTIONS AND MATRIX ELEMENTS

Many nuclear levels in the  $A = 17-39$  region can be described in terms of an "sd-shell" shell model, in which eight neutrons and eight protons are confined to the (filled)  $0s$  and  $0p$  orbits and the remaining, active, nucleons occupy the  $1s$  and  $0d$  orbits, of  $n, l, j$  values  $1s_{1/2}$ ,  $0d_{5/2}$  and  $0d_{3/2}$ . Recent calculations within this "sd" model space have produced wave functions from a unified formulation of the model hamiltonian which have been quite successful in reproducing the binding energies and excitation energies for nuclei with  $8 < N, Z < 20$  [ref. <sup>6</sup>]. These wave functions span the complete spaces of  $0d_{5/2}$ ,  $1s_{1/2}$ , and  $0d_{3/2}$  configurations, which is a critical aspect when considering matrix elements of operators, such as the spin operator, for which the transitions between the spin-orbit partners are of paramount importance <sup>7</sup>). With these wave functions it is possible to analyze systematically experimental M1 and Gamow-Teller data from the sd-shell with a minimum of concern for the effects of varying space truncations and hamiltonian formulations which vitiate most quantitative shell-model analyses of heavier nuclei.

The shell-model calculations upon which the present predictions are based assumed the constraint of a hamiltonian which conserves isospin. This hamiltonian is limited to one- and two-body interactions and, more specifically, has a fixed one-body spectrum and a single set of two-body matrix elements. These two-body matrix elements are scaled for application to a given  $A$ -value by the factor  $(18/A)^{0.3}$ . Hamiltonian matrices based on these parameters were diagonalized to produce a family of wave functions  $|NTJn\rangle$ , where  $N = A - 16$ ,  $T$  and  $J$  designate the total isobaric and angular momentum spin values, and  $n$  is the counting index which identifies a particular eigenstate of the  $NTJ$  set.

The reduced matrix element between multiparticle shell-model wave functions of any one-body operator  $O^{(\Delta J, \Delta T)}$ , of tensor rank  $\Delta J$  in angular momentum space and tensor rank  $\Delta T$  in isospin space, can be expressed as a sum of the products of the elements of the multiparticle transition amplitudes ( $D$ ) times single-particle matrix elements ( $S$ ), where the sum runs over all single-particle states [see ref. <sup>8</sup>]

$$\langle f || O^{(\Delta J, \Delta T)} || i \rangle = \sum_{j, j'} D(\Delta J, \Delta T, j, j', f, i) S(O^{(\Delta J, \Delta T)}, j, j'), \quad (1)$$

where

$$D(\Delta J, \Delta T, j, j', f, i) = [(2\Delta J + 1)(2\Delta T + 1)]^{-1/2} \\ \times \langle f || [a^+(j) \otimes a^-(j')]^{(\Delta J, \Delta T)} || i \rangle, \quad (2)$$

$$S(O^{(\Delta J, \Delta T)}, j, j') = \langle j || O^{(\Delta J, \Delta T)} || j' \rangle. \quad (3)$$

The initial and final multiparticle states are denoted by  $|i\rangle$  and  $|f\rangle$ , respectively, and “ $j$ ” is used to represent the full set of single-particle quantum numbers ( $n, l, j$ ). The operator  $a^+(j)$  creates a particle in orbit  $j$  and the operator  $a^-(j')$  destroys a particle in orbit  $j'$ . Hence, the theoretical matrix elements are obtained from a sum of products of the multiparticle matrix elements of  $a^+(j) \otimes a^-(j')$  as evaluated with the shell-model wave functions of ref. <sup>6)</sup> and the single-particle matrix elements of the M1 operator for the sd-shell orbits.

For the sd-shell model space there are ten independent single-particle matrix elements, corresponding to the  $j-j'$  combinations  $0d_{5/2}-0d_{5/2}$ ,  $0d_{5/2}-0d_{3/2}$ ,  $1s_{1/2}-1s_{1/2}$ ,  $1s_{1/2}-0d_{3/2}$  and  $0d_{3/2}-0d_{3/2}$  for the  $\Delta T=0$  (isoscalar) and  $\Delta T=1$  (isovector) couplings. (The  $j-j'$  and  $j'-j$  terms can be combined for each pair of inequivalent orbits.) The corresponding multiparticle transition amplitudes  $D$  are uniquely and completely determined by the specification of the model hamiltonian and embody its entire predictive contents for rank-one operators.

The values of the  $D$  amplitudes for the transitions and moments we consider in this work are given in refs. <sup>4,9)</sup>. The high degree of configuration mixing predicted by the present shell-model calculations can be seen in these  $D$ -values in the significant contributions of several single-particle paths to a typical transition. These individual components, from which the net theoretical strengths are constructed, are basic to detailed theoretical considerations of M1 and Gamow-Teller phenomena. Evaluations of predictions of orbit-dependent renormalizations, for example, require knowledge of the contributions from these individual orbits.

## 2.2. FORMULATION FOR THE FREE-NUCLEON M1 OPERATOR

The M1 operator  $O(M1)$  can be written in terms of its isoscalar (IS) and isovector (IV) components as

$$O(M1) = \frac{1}{2}[O(ISM1) + O(IVM1)], \quad (4)$$

where

$$\begin{aligned} O(ISM1) &= (3/4\pi)^{1/2} \sum_k [g_s(ISM1)s^k + g_l(ISM1)l^k] I(IS)\mu_N, \\ O(IVM1) &= (3/4\pi)^{1/2} \sum_k [g_s(IVM1)s^k + g_l(IVM1)l^k] I(IV)\mu_N, \end{aligned} \quad (5)$$

where  $I(IS) = 1$  and  $I(IV) = \tau^k$  and  $\mu_N$  is the nuclear magneton. The sum is over the nucleons in the nucleus and the  $g$ 's are the spin and orbital  $g$ -factors for the free nucleons:

$$\begin{aligned} g_s(ISM1) &= \frac{1}{2}[g_s(\text{proton}) + g_s(\text{neutron})] = 0.880, \\ g_l(ISM1) &= \frac{1}{2}[g_l(\text{proton}) + g_l(\text{neutron})] = 0.500, \\ g_s(IVM1) &= \frac{1}{2}[g_s(\text{proton}) - g_s(\text{neutron})] = 4.706, \\ g_l(IVM1) &= \frac{1}{2}[g_l(\text{proton}) - g_l(\text{neutron})] = 0.500. \end{aligned} \quad (6)$$

The matrix element of the M1 operator reduced in angular-momentum space can be expressed as a sum over the matrix elements reduced in both angular-momentum and isospin space

$$\begin{aligned}
 M(\mathbf{M1}) = \langle f \| O(\mathbf{M1}) \| i \rangle &= \left(\frac{1}{2}\right)(-1)^{T_f - T_i} \\
 &\times \left[ \begin{pmatrix} T_f & 0 & T_i \\ -T_z & 0 & T_z \end{pmatrix} \langle f \| O(\text{ISM1}) \| i \rangle \right. \\
 &\left. + \begin{pmatrix} T_f & 1 & T_i \\ -T_z & 0 & T_z \end{pmatrix} \langle f \| O(\text{IVM1}) \| i \rangle \right]. \quad (7)
 \end{aligned}$$

Our reduced matrix element convention is that of Edmonds<sup>10</sup>).

In terms of these reduced matrix elements, magnetic moments are given by

$$\begin{aligned}
 \mu &= (4\pi/3)^{1/2} \langle i, J_z = J | O(\mathbf{M1}) | i, J_z = J \rangle \\
 &= (4\pi/3)^{1/2} [J/(J+1)(2J+1)] \langle i \| O(\mathbf{M1}) \| i \rangle, \quad (8)
 \end{aligned}$$

and the reduced transition probability for M1 transitions is given by

$$B(\mathbf{M1}) = [\langle f \| O(\mathbf{M1}) \| i \rangle]^2 / (2J_i + 1). \quad (9)$$

### 2.3. FORMULATION FOR THE EFFECTIVE M1 OPERATOR

There are several reasons why even “perfect” shell-model calculations of electromagnetic matrix elements based on the free-nucleon characteristics of the neutron and proton should differ from the corresponding experimental values. In reality, the nuclear wave functions must be more complicated than those of the theoretical model we use. Real nuclear states must involve nucleonic degrees of freedom beyond the sd-shell space. In addition, non-nucleonic degrees of freedom which involve delta isobars and mesons may be important in the observed phenonema.

The corrections to the standard shell-model predictions which arise from these sources have been the subject of many theoretical investigations [refs. <sup>2,3</sup>]. The complexity of the theory leaves considerable ambiguity in conclusions about the relative importance of the many paths for renormalization effects. In particular, there are conflicting estimates concerning the relative importance of the delta isobar correction <sup>2,3,11,12</sup>).

Our approach to this problem is to attempt to extract “empirical” corrections to the free-nucleon M1 operator by examining the relationships between experimental data and the predictions of large-basis shell-model calculations which are confined to the standard limits of one major oscillator shell.

We assume that the corrections to these predictions for all the higher-order contributions to the observed matrix element values can be incorporated into a renormalization of the single-particle matrix elements of the M1 operator. Since the

most general effective operator can be expressed in terms of the ten single-particle matrix elements given above (sect. 2.1) and since there are many experimental data, empirical values for the renormalization of these matrix elements can be found from a least-squares fit of the theoretical expressions to the experimental data.

The detailed procedure by which the empirical corrections to the values of the single-particle matrix elements are obtained follows that of ref. <sup>1</sup>). The renormalized single-particle matrix elements can be expressed in terms of  $\delta$ -parameters associated with an effective M1 operator which we write in the form

$$O^{\text{eff}}(\text{ISM1}/\text{IVM1}) = (3/4\pi)^{1/2} [g_s \mathbf{S} + g_l \mathbf{L} + g_s \delta(\text{M1})] \mu_N, \quad (10)$$

where

$$\delta(\text{M1}) = \delta_s(\text{M1}, d-d) \mathbf{S}(d-d) + \delta_s(\text{M1}, s-s) \mathbf{S}(s-s) + \delta_l(\text{M1}, d-d) \mathbf{L}(d-d) \\ + \delta_p(\text{M1}, d-d) \mathbf{P}(d-d) + \delta_p(\text{M1}, s-d) \mathbf{P}(s-d), \quad (11)$$

$$\mathbf{S}(d-d) = \sum_{d-d} s^k I(\text{IS}/\text{IV}),$$

$$\mathbf{S}(s-s) = \sum_{s-s} s^k I(\text{IS}/\text{IV}),$$

$$\mathbf{L}(d-d) = \sum_{d-d} l^k I(\text{IS}/\text{IV}),$$

$$\mathbf{P}(s-d) = \sum_{s-d} p^k I(\text{IS}/\text{IV}),$$

$$\mathbf{P}(d-d) = \sum_{d-d} p^k I(\text{IS}/\text{IV}), \quad (12)$$

$$p^k = (8\pi)^{1/2} [Y^{(2)}(\mathbf{r}^k) \otimes s^k]^{(1)}. \quad (13)$$

The  $\delta$ -coefficients characterize the (IS/IV)-dependent renormalizations [denoted by  $\delta_s(\text{ISM1})$  and  $\delta_l(\text{IVM1})$ , respectively] which are needed when working within the shell-model space. The notation (d-d), (s-d) and (s-s) identifies the respective pairs of orbits,  $l=2$  ( $0d_{5/2}$  and  $0d_{3/2}$ ) and  $l=0$  ( $1s_{1/2}$ ) which are acted on by the operators. The total operators are given by

$$\mathbf{S} = \mathbf{S}(d-d) + \mathbf{S}(s-s), \\ \mathbf{L} = \mathbf{L}(d-d), \\ \mathbf{P} = \mathbf{P}(d-d) + \mathbf{P}(s-d). \quad (14)$$

The reduced single-particle matrix elements for the individual operator components  $s$ ,  $l$  and  $p$  and the explicit relationship between the effective sd-shell single-particle matrix elements and the  $\delta$  parameters are given in ref. <sup>1</sup>).

We note that there are two  $\delta_p$  parameters in eq. (11), one associated with the diagonal  $l=2$  matrix elements and the other associated with the  $l$ -forbidden  $s_{1/2}$  to  $d_{3/2}$  matrix element. These  $\delta$ -parameters are relatively poorly determined in the least-squares fits to be discussed below. However, the values of  $\delta p(d-d)$  and  $\delta p(s-d)$  are theoretically rather similar [ref. <sup>1</sup>]. Thus, we are led to combine the two  $\delta_p$  parameters into a single parameter  $\delta_p$  by considering the combined operator

$$\delta_p \mathbf{P} = \delta_p(d-d) \mathbf{P}(d-d) + \delta_p(s-d) \mathbf{P}(s-d). \quad (15)$$

All of the results discussed below will be in terms of this eight-parameter formulation for the effective M1 operator, namely four parameters each,  $\delta_s(d-d)$ ,  $\delta_s(s-s)$ ,  $\delta_t(d-d)$  and  $\delta_p$ , for the isoscalar and isovector components.

We expect some mass dependence in the value of the  $\delta$  parameters since the renormalizations are theoretically somewhat different for the particle states in  $A=17$  and the hole states in  $A=39$  [ref. <sup>2</sup>]. We will assume that this mass dependence is smooth and parametrize it in the form

$$\delta(A) = \delta(A=28)(A/28)^X. \quad (16)$$

The rms deviation between the experimental and theoretical M1 matrix elements changes little over the range  $X=0$  to 1 due to a correlation between  $X$  and the  $\delta$ -parameters. We have chosen a value of  $X=0.35$  based on the calculated values for  $A=16$  and 40 of Towner and Khanna [refs. <sup>1,2</sup>]. (In principle, one should also introduce effective many-body operators for  $A=18-38$ ; however, empirically there appears to be little need for them beyond that incorporated implicitly into the mass dependence.)

### 3. Experimental data set and comparison with shell-model values

Empirical values for the  $\delta$ -parameters defined in sect. 2.3 have been determined by making least-squares fits of shell-model densities to various subsets of all relevant experimental data from sd-shell nuclei. We have previously considered the isoscalar and isovector M1 moments and the Gamow-Teller "beta moments" of the "mirror-level" data set consisting of mirror states whose magnetic moments and interconnecting Gamow-Teller beta decays were measured [ref. <sup>1</sup>]. These include the ground states of the nine  $T=\frac{1}{2}$  pairs with  $A=17, 19, 21, 25, 27, 29, 31, 35$  and 39. A similar analysis was also applied to the set of all GT beta decay data in the sd-shell for which experimental errors in the matrix elements are 10% or less [189 data, ref. <sup>4</sup>].

In this paper we consider a fit to a more comprehensive set of sd-shell data related to the M1 operator. We consider both magnetic moments <sup>13</sup>) (49 data) and M1 transitions <sup>14</sup>) whose associated matrix elements have been measured to an accuracy of 10% or better (114 data). In addition to the data covered by ref. <sup>13</sup>), we include the recent measurement of the <sup>33</sup>Cl magnetic moment by Rogers *et al.* <sup>15</sup>). The magnetic moments and  $B(M1)$  values are converted into reduced M1 matrix elements using eqs. (8) and (9). These matrix elements, expressed in terms of the isoscalar and isovector  $\delta$ -parameters via eqs. (7) and (10), are then used to determine the best values for the  $\delta$ -parameters by a least-squares fit.

A summary of the data sets and the resulting  $x$  values obtained in the least-squares fits is given in table 1. Each matrix element [as defined in eq. (7)] was weighted in the least-squares fit by an "error" which consisted of a theoretical error of  $0.1 \mu_N$  added in quadrature with the experimental error. This theoretical error was chosen to make the  $x$  value on the order of unity and is introduced to give a more equitable

TABLE 1  
Data sets and  $x$  values for the least-squares fits for the effective M1 operator

| Data set                                     | Number of data | Number of parameters | $x$ free nucleon operator | $x$ fitted operator |
|--|----------------|----------------------|---------------------------|---------------------|
| mirror-level isoscalar moments <sup>a)</sup> | 15             | 4                    |                           |                     |
| mirror-level isovector moments <sup>a)</sup> | 12             | 4                    |                           |                     |
| all moments <sup>b)</sup>                    | 49             | 8                    | 1.64                      | 0.99                |
| all M1 decay <sup>b)</sup>                   | 114            | 7                    | 2.16                      | 1.58                |
| moments plus M1 decay <sup>b)</sup>          | 163            | 8                    | 2.00                      | 1.43                |

The  $x$  values include a theoretical error of  $0.1 \mu_N$  for the M1 matrix element which was added in quadrature to the experimental error (see text sect. 3).

<sup>a)</sup> Ref. <sup>1)</sup>.

<sup>b)</sup> Present work.

weighting to each datum, and as well, to assign a realistic error to the resulting  $\delta$ -parameters. In those fits for which  $x$  differs from unity, the errors obtained in the fits for the  $\delta$ -parameters were multiplied by  $x$  before being entered in table 2.

### 3.1. EMPIRICAL VALUES OF THE $\delta$ -PARAMETERS

The  $\delta$ -parameters obtained from the eight parameter fits for the effective operator are given in table 2, along with the results we obtained previously from the analysis of the mirror-level data of ref. <sup>1)</sup>. We note first that the isoscalar parameters are less well determined from the present fit than they were from the fit to the pure isoscalar moments derived from the mirror-level data. Presumably this is because the uncertainties in the present fit are dominated by the experimental and (more so) the theoretical errors in the larger isovector contributions. When the isoscalar moments of the mirror-level data are considered in isolation, the uncertainty in the theoretical isovector part does not enter of course, and the values and uncertainties of the isoscalar parameters arise only from the internal consistency of isoscalar comparison. Hence, we conclude that this previous determination of the  $\delta$ (ISM1) values is superior to that obtained in the present solution, and we use them in the remaining discussion and for figs. 1-4.

The isovector parameters are better determined from the present data set than they were from the mirror-level isovector data. A particular case in point is the  $\delta_s(s-s)$  term, which in the mirror-level fit had a small and relatively uncertain value. This was due to the fact that it was determined primarily from the only two data which had an appreciable  $0s_{1/2}-0s_{1/2}$  single-particle term, namely the isovector moments of the  $T = \frac{1}{2}$  ground states of  $A = 29$  and  $A = 31$ . In the present data set there are a number of transitions which have relatively large contributions from



TABLE 2  
Empirical values of the  $\delta$ -parameters scaled to  $A = 28$

| Data set   | $\delta_s(d-d)$ | $\delta_s(s-s)$ | $\delta_t$         | $\delta_p$ |
|--|-----------------|-----------------|--------------------|------------|
| <i><math>\delta(IS)</math> for the isoscalar spin operator <sup>a)</sup></i> |                 |                 |                    |            |
| mirror-level moments <sup>b)</sup>   | -0.32 (5)       | -0.13 (9)       | 0.050 (9)          | 0.08 (6)   |
| all moments  | -0.37 (16)      | 0.05 (30)       | 0.083 (25)         | 0.23 (19)  |
| all M1 decay   | -0.25 (25)      | 0.12 (49)       | 0.05 <sup>c)</sup> | 0.09 (23)  |
| moments plus M1 decay  | -0.25 (13)      | 0.03 (26)       | 0.065 (23)         | 0.12 (13)  |
| <i><math>\delta(IVM1)</math> for the isovector M1 operator</i>               |                 |                 |                    |            |
| mirror-level moments <sup>b)</sup>   | -0.116 (33)     | -0.001 (42)     | 0.013 (8)          | 0.022 (30) |
| all moments  | -0.102 (19)     | -0.032 (24)     | 0.017 (3)          | 0.043 (15) |
| all M1 decay   | -0.153 (22)     | -0.138 (33)     | 0.026 (6)          | 0.088 (13) |
| moments plus M1 decay  | -0.149 (13)     | -0.099 (20)     | 0.023 (3)          | 0.081 (9)  |
| <i><math>\delta(GT)</math> for the Gamow-Teller operator</i>                 |                 |                 |                    |            |
| mirror-level GT decay <sup>b)</sup>  | -0.276 (20)     | -0.227 (26)     | 0.004 (4)          | 0.018 (16) |
| all GT decay   | -0.248 (11)     | -0.226 (16)     | 0.004 (3)          | 0.017 (8)  |

The values obtained from the mirror-level data <sup>1)</sup> are compared to the results of the present fit to all M1 transitions and magnetic moments and to the fit to all GT transitions <sup>4)</sup>.

<sup>a)</sup> We give the here the  $\delta$ -parameters for the isoscalar matrix elements  $\langle S \rangle$  which are denoted by  $\delta(IS)$  in ref. <sup>1)</sup> and fig. 5. The  $\delta$ -parameters for the total isoscalar M1 operator, denoted by  $\delta(ISM1)$  in ref. <sup>1)</sup> are related to  $\delta(IS)$  by the relation  $\delta(ISM1) = \{ [g_s(ISM1) - g_t(ISM1)] / g_s(ISM1) \} \delta(IS) = 0.432 \delta(IS)$ .

<sup>b)</sup> From the "A = 18 - 38, (A/28)<sup>0.35</sup> mass-dependent" fit given in table 4 of ref. <sup>1)</sup>.

<sup>c)</sup> Since M1 transitions only depend on the linear combination of operators  $S$  plus  $L$ , the  $\delta$ -parameter for the orbital part was fixed to be close to the value obtained in the mirror-level fit.

$0s_{1/2} - 0s_{1/2}$ , and the new value for  $\delta_s(s-s)$  is more representative of typical sd-shell structure.

We note also that the  $\delta_p$  parameter was not well determined in the previous, mirror-level fit. There are about a dozen M1 transitions for which the  $\delta_p$  parameter is important; most of these involve the  $l$ -forbidden,  $0s_{1/2} - 1d_{3/2}$ , term. Thus, the present value for  $\delta_p$  is again more representative of the typical sd-shell data. (The  $A = 39$ ,  $\frac{1}{2}^+ \rightarrow \frac{3}{2}^+$  transition considered in ref. <sup>16)</sup> is a pure  $0s_{1/2}$  to  $1d_{3/2}$  transition in our model. However, we do not include this transition in the present fit because the matrix elements have an experimental uncertainty larger than 10%. The comparison with this  $A = 39$  transition will be discussed in sect. 4.

We have expressed our effective operators in a formulation which is closely related to their underlying microscopic origins. In order to compare with the more traditional parametrizations, it is worthwhile to express our results in terms of the effective spin and orbital  $g$ -factors. If we assume that  $\delta_s$  and  $\delta_p$  are orbit independent, then eq. (10) can be written in terms of effective  $g$ -factors:

$$O(ISM1/IVM1) = (3/4\pi)^{1/2} \sum_k [g_s^{\text{eff}} s^k + g_t^{\text{eff}} I^k + g_p^{\text{eff}} p^k] I(IS/IV) \mu_N. \quad (17)$$

The  $g^{\text{eff}}$  are the (IS/IV)- and  $A$ -dependent effective  $g$ -factors given in terms of the

TABLE 3

Effective  $g$ -factors defined by eq. (18) evaluated with the  $\delta$ -parameters for the d-orbit obtained from the isoscalar M1 "mirror-level moments" fit and the isovector M1 "moments plus M1 decay" fit as given in table 2

|       |           | Free-nucleon | Effective |        |        |
|-------|-----------|--------------|-----------|--------|--------|
|       |           |              | A = 17    | A = 28 | A = 39 |
| $g_s$ | isoscalar | 0.880        | 0.78      | 0.76   | 0.74   |
|       | isovector | 4.706        | 4.12      | 4.00   | 3.92   |
|       | proton    | 5.586        | 4.90      | 4.76   | 4.66   |
|       | neutron   | -3.826       | -3.34     | -3.25  | -3.18  |
| $g_t$ | isoscalar | 0.50         | 0.516     | 0.519  | 0.521  |
|       | isovector | 0.50         | 0.591     | 0.608  | 0.622  |
|       | proton    | 1.00         | 1.107     | 1.127  | 1.143  |
|       | neutron   | 0.00         | -0.075    | -0.089 | -0.100 |
| $g_p$ | isoscalar | 0            | 0.03      | 0.03   | 0.03   |
|       | isovector | 0            | 0.32      | 0.38   | 0.43   |
|       | proton    | 0            | 0.35      | 0.41   | 0.46   |
|       | neutron   | 0            | -0.29     | -0.35  | -0.39  |

(IS/IV)-dependent free-nucleon  $g$ -factors and the (IS/IV)- and  $A$ -dependent  $\delta$ -parameters by:

$$g_s^{\text{eff}}(A) = g_s + g_s \delta_s(M1A = 28)(A/28)^{0.35},$$

$$g_t^{\text{eff}}(A) = g_t + g_t \delta_t(M1A = 28)(A/28)^{0.35},$$

and

$$g_p^{\text{eff}}(A) = g_s \delta_p(M1A = 28)(A/28)^{0.35}. \tag{18}$$

In table 3 we give the effective  $g$ -factors for  $A = 17, 28$  and  $39$  evaluated with the  $\delta$ -parameters for the d-orbit obtained from the isoscalar "mirror-level moments" fit and the isovector "moments plus M1 decay" fit as given in table 2. Note that the values of  $\delta(\text{IS})$  given in table 2 must be multiplied by 0.432 in order to obtain the  $\delta(\text{ISM1})$  which should be used in eq. (18) (see footnote to table 2). The proton and neutron  $g$ -factors given in table 3 are related to the isospin-dependent  $g$ -factors by the inverse of eq. (6), i.e.

$$g(\text{proton}) = g(\text{ISM1}) + g(\text{IVM1}),$$

$$g(\text{neutron}) = g(\text{ISM1}) - g(\text{IVM1}). \tag{19}$$

### 3.2. COMPARISON OF EXPERIMENTAL AND THEORETICAL MULTIPARTICLE M1 MATRIX ELEMENTS

Experimental and theoretical M1 transition matrix elements are compared in fig. 1 and the magnetic moments are compared in fig. 2. In each figure the plotted points

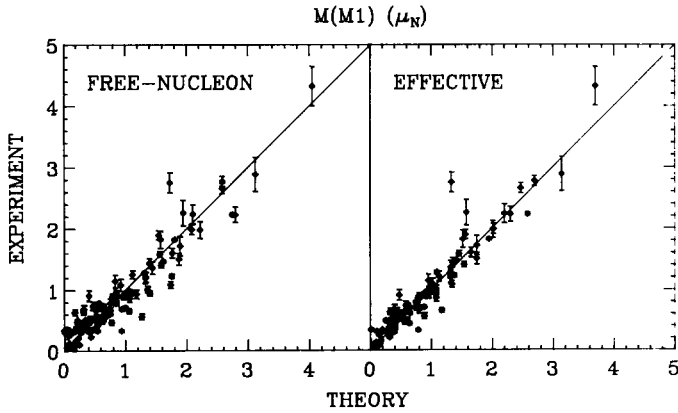


Fig. 1. Theoretical versus experimental M1 transition matrix elements. The plotted points have y-coordinates corresponding to the experimental value of a matrix element and x-coordinates corresponding to the matching theoretical matrix element. Exact agreement between experiment and theory corresponds to points which lie on the 45° lines drawn in the figure. On the left-hand side the experimental values are matched with calculations based on the free-nucleon formulation of the M1 operator. On the right-hand sides the experimental values are matched with the calculations based on the effective M1 operator.

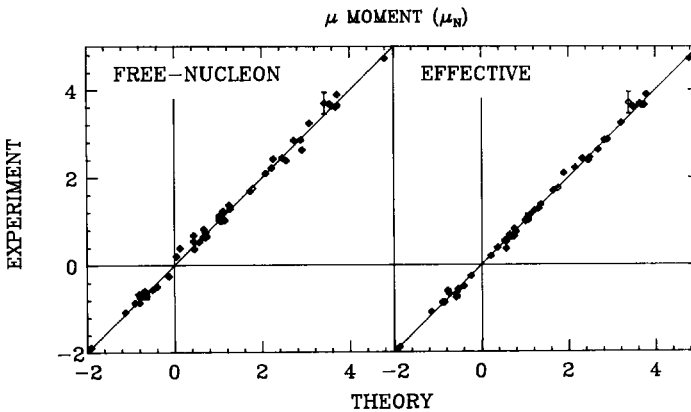


Fig. 2. Theoretical versus experimental magnetic moments. See caption to fig. 1.

have y-coordinates corresponding to the experimental value of a matrix element and x-coordinates corresponding to the matching theoretical matrix element. Exact agreement between experiment and theory corresponds to points which lie on the 45° lines drawn in the figures. On the left-hand sides of figs. 1 and 2, the experimental values are matched with calculations based on the free-nucleon formulation of the M1 operator (sect. 2.2). On the right-hand sides of the figures, experimental values are matched with the calculations based on the effective M1 operator.

As noted, the isovector and isoscalar components of the M1 operator can be isolated by looking at the difference and sum, respectively, of the matrix elements

for mirror moments:

$$\begin{aligned} \mu_1 &= \frac{1}{2}[\mu(T_z = T) - \mu(T_z = -T)], \\ \mu_0 &= \frac{1}{2}[\mu(T_z = T) + \mu(T_z = -T)]. \end{aligned} \tag{20}$$

The isovector moments are plotted in fig. 3. In fig. 4 we plot the isoscalar spin matrix element  $\langle S \rangle$  obtained from the isoscalar moments by the relation <sup>1)</sup>

$$\langle S \rangle = (\mu_0 - \frac{1}{2}J) / 0.38. \tag{21}$$

In our analysis of GT beta-decay <sup>4)</sup> we observed that the theoretical multiparticle matrix elements calculated with the free-nucleon GT operator were, obviously and significantly, larger than the corresponding experimental values. In order to obtain

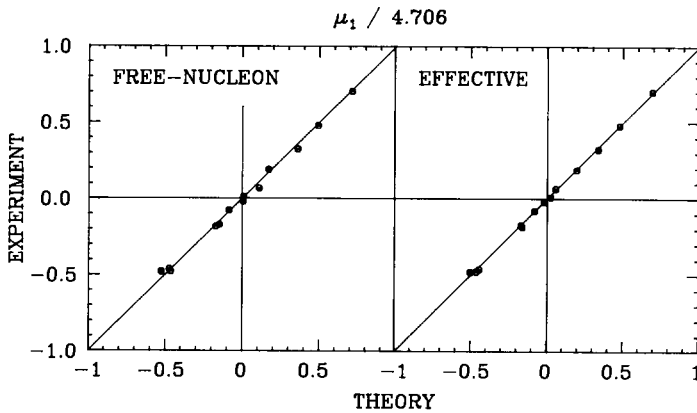


Fig. 3. Theoretical versus experimental isovector M1 matrix elements. See caption to fig. 1.

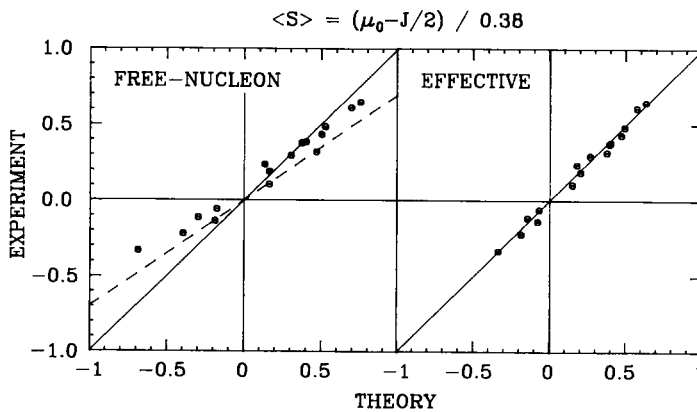


Fig. 4. Theoretical versus experimental isoscalar spin matrix elements,  $\langle S \rangle$ . See caption to fig. 1. The dashed line on the left-hand side corresponds to the "best" quenching (rotation) of the calculated values.

agreement with experiment, the free-nucleon GT matrix elements of operators had to be “quenched” by a factor of about 0.77 (corresponding to a “quenching” of about 0.60 in the strength, or matrix element squared). In contrast to this GT result, there appears to be no obvious need for quenching of the free-nucleon calculation for the M1 matrix elements shown in figs. 1, 2 and 3. However, the scatter of the points about the 45° line is reduced with the effective operator. Indeed, the quantitative agreement of experimental magnetic moments with the effective-operator theory, fig. 2, is quite impressive. (More details of the results for M1 transitions will be presented in ref. <sup>14</sup>.)

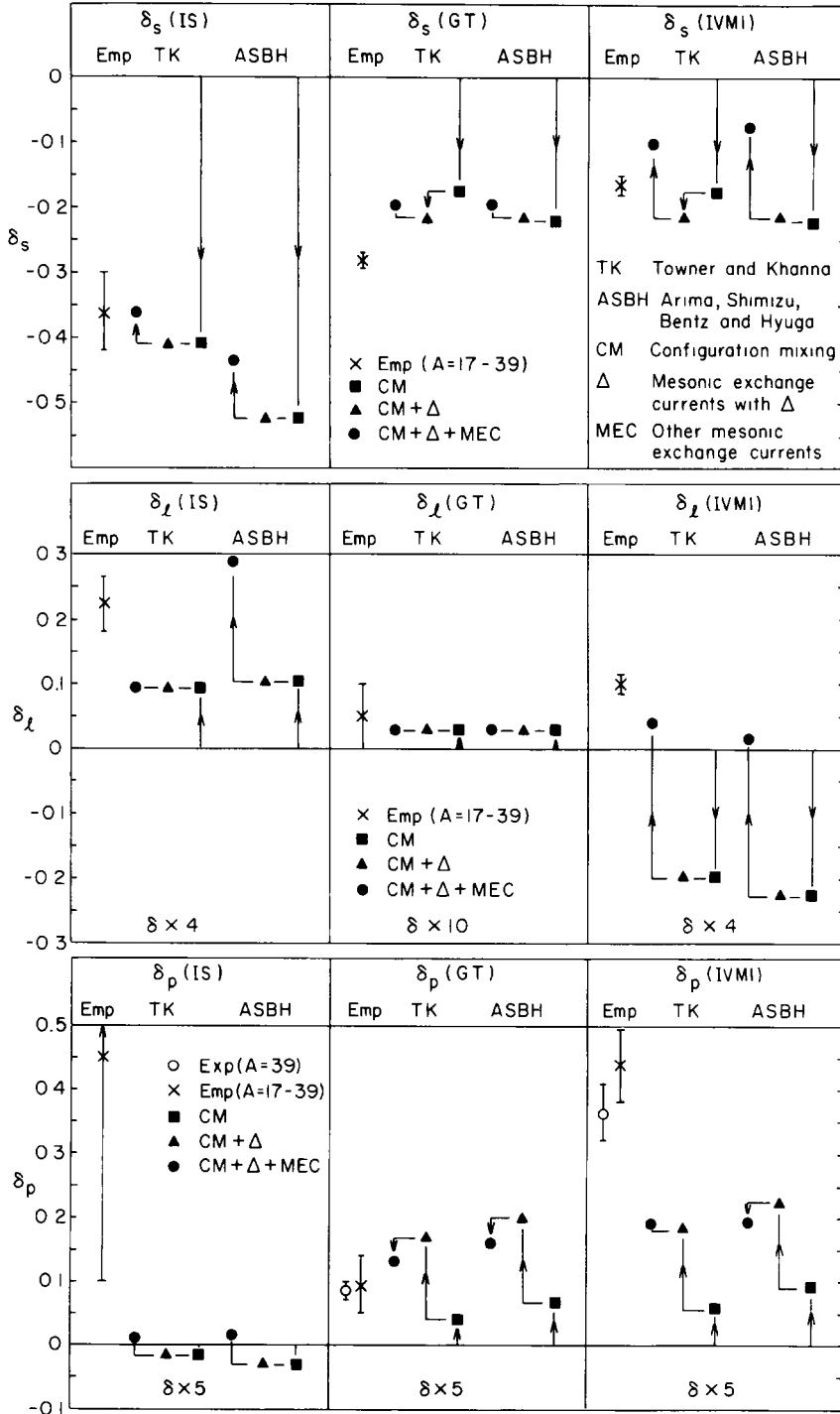
This apparent difference between GT and M1 matrix elements arises from two sources. One is that the isovector M1 operator, with its orbital component, is more complicated than the GT operator. The quenching of the M1 spin contribution is partially cancelled by a compensating enhancement in the orbital contribution. The other is that, empirically, there is indeed less quenching of the M1 spin operator than of the GT spin operator, reflected in the values of the  $\delta_s$  parameter given in table 2. In sect. 4. We will see that this can be understood by the presence of additional exchange currents for the effective M1 operator.

The isoscalar data, which are compared with theory in fig. 4, show considerable deviations from the free-nucleon values. The deviations cannot be explained by a simple overall quenching, which would correspond to the rotated dashed line on the left-hand side of fig. 4. Both the  $\delta_s$  and  $\delta_l$  components of the effective isoscalar operator are important. The effective operator derived from isoscalar moments is consistent with the quenching found for isoscalar M1 transitions <sup>17,14</sup>).

#### 4. Theoretical foundations

In fig. 5 our empirical values for the  $\delta$ -parameters are compared with recent theoretical calculations of these parameters based on a consideration of higher-order configuration mixing and mesonic-exchange currents for single-particle states around <sup>40</sup>Ca. The empirical values derived from the present results discussed in sect. 3.1 are scaled to  $A = 39$  by the assumed mass dependence  $\delta(A) = \delta(A = 28)(A/28)^{0.35}$  and are compared to the calculations based on one hole in a <sup>40</sup>Ca closed-shell configuration. In addition to the results for the M1 operator discussed above, we also include in fig. 5 comparisons of the GT operator based on ref. <sup>4</sup>). The  $\delta_s$  values used for the figure are those for the d-orbit,  $\delta_s(d-d)$ .

The calculated values are taken from the works of Towner and Khanna (TK) <sup>2</sup>) and Arima, Shimizu, Bentz and Hyuga (ASBH) <sup>3</sup>). The corrections are broken down into three components: (i) those arising from high-order configuration mixing (CM), (ii) those arising from mesonic-exchange currents involving the  $\Delta$ -isobar, and (iii) those arising from other mesonic-exchange currents such as the one-pion exchange and the pionic-pair diagrams (MEC). It is important to remember that the first-order configuration mixing which dominates the non-sd-shell corrections for operators



such as the electric quadrupole operator are not present for the M1 and GT operators, since these later have no radial dependence.

A number of interesting conclusions can be drawn from the comparisons of our empirical results with these theoretical predictions. The empirical value of  $\delta_s(\text{IS})$  derived from isoscalar moments is quite large and is in good agreement with both calculations. The calculated quenching comes mostly from CM with a little enhancement from MEC— the  $\Delta$ -isobar contributions vanish in this case because the particle-hole vertex must change isospin by one unit.

The empirical value of  $\delta_s(\text{GT})$  is about 50% larger than the calculated values. Again, the calculated quenching comes mostly from CM. For both  $\delta_s(\text{IS})$  and  $\delta_s(\text{GT})$  the CM contribution is dominated by the tensor interaction, and the ratio  $\delta_s(\text{GT, CM})/\delta_s(\text{IS, CM}) \approx 0.42$  is insensitive to details of the CM calculation<sup>3)</sup>. Thus, with CM alone it is difficult to explain the additional empirical GT quenching without destroying the agreement for the isoscalar moments.

The importance of the  $\Delta$ -contribution to  $\delta_s(\text{GT})$ , however, remains controversial after many calculations [table 4 in ref. <sup>1)</sup> and references therein]. For example, Oset and Rho<sup>12)</sup> obtain  $\delta_s(\text{GT}, \Delta) = -0.15$ , as compared to  $-0.038$  from Towner and Khanna and to  $0.004$  from Arima *et al.* Such differences arise from the assumptions made about short-range correlations, exchange terms and crossing terms. Agreement with our empirical value would be obtained with  $\delta_s(\text{GT}, \Delta) \approx -0.10$ , a value intermediate to the extremes of the predictions. We note that the agreement to  $\delta_s = -0.10$  can be improved within the model of Oset and Rho by using a more recent estimate of the Landau parameter  $g'_{\Delta}$  [ref. <sup>18)</sup>]. Thus, we propose that the “quenching” observed for the Gamow-Teller operator comes about approximately  $\frac{2}{3}$  from higher-order configuration mixing and  $\frac{1}{3}$  from  $\Delta$ -admixture.

The predicted values of  $\delta_s$  for the GT and the isovector M1 (IVM1) operators differ only in the MEC component. The CM and  $\Delta$  corrections each contribute equally to GT and IVM1 because the corrections are dominated by the (nonrelativistic)  $\sigma\tau$  operator in both cases. On the other hand, the MEC contribution depends upon the underlying relativistic structure, i.e. axial-vector for GT and vector for M1. It turns out the MEC corrections for the GT operator, which arise mainly from the  $\rho - \pi$  diagram, are small relative to the one-pion exchange contribution for the

---

Fig. 5. Empirical  $\delta$ -parameters (scaled to  $A = 39$ ) compared to recent calculations. The empirical (Emp) values are plotted on the left-hand side of each panel with a cross and error bar. These are based on the results listed in table 2: the “mirror-level moments” fit for  $\delta(\text{IS})$ , the “moments plus M1 decay” fit for  $\delta(\text{IVM1})$  and the “all GT decay” fit for  $\delta(\text{GT})$ . The empirical isovector  $\delta_p$  parameters based on the  $A = 39$   $\frac{1}{2}^+ \rightarrow \frac{3}{2}^+$  transitions<sup>16)</sup> (with assumed positive signs) are plotted with an open circle and error bar. The calculated values are from Towner and Khanna (TK) and from Arima *et al.* (ASBH). The total calculated value (CM +  $\Delta$  + MEC) for each parameter is given by the filled circle. Individual components are also shown for CM (filled squares) and for CM +  $\Delta$  (filled triangles). The various theoretical components are connected by lines with arrows in order to guide the eye.

M1 operator. The empirical difference  $\delta_s(\text{IVM1}) - \delta_s(\text{GT}) \approx 0.12$  is in fair agreement with the MEC calculations.

The empirical values of  $\delta_l$  in fair agreement with the predictions. The early versions of the relativistic  $\sigma$ - $\omega$  model<sup>19)</sup> appeared to give extremely large corrections to the M1 orbital operator, as a consequence of the  $M^*/M$  factor<sup>20)</sup>. In fact, this was one of the early reasons for rejecting such models. For the isoscalar moments it now appears that there are nuclear-medium corrections, “backflow” diagrams, which bring the result back close to the nonrelativistic model<sup>21,22,3,23)</sup>. The situation for the isovector moments is not so clear<sup>23)</sup>.

The empirical value for  $\delta_l(\text{IS})$  is about twice as large as the calculated CM contribution. Predictions which incorporate the addition of new calculations for the MEC by Arima *et al.* somewhat overshoot the empirical value. For  $\delta_l(\text{IVM1})$  the agreement between experiment and theory seems good in the light of the very large cancellation between the CM and MEC contributions. There still seems to be room for some “relativistic” corrections<sup>23)</sup> for the IVM1 orbital  $g$ -factor.

The  $\delta_p$  comparison in fig. 5 includes values derived from the “single-particle”  $\frac{3}{2}^+$  to  $\frac{1}{2}^+$  transitions in  $A = 39$  [ref. 16)] which are consistent with those obtained in our global ( $A = 17$ – $39$ ) analysis. The large error in the empirical  $\delta_p(\text{IS})$  value precludes any meaningful comparison with the small theoretical corrections. The calculated  $\delta_p$  corrections for GT and IVM1 are similar in value and dominated by the  $\Delta$ -isobar correction. The agreement for GT is good, but the empirical correction for the isovector M1 transitions is nearly twice as large as that calculated. At present this discrepancy is not understood.

## 5. Conclusions and summary

This paper completes a series of works in which we have attempted to characterize the nature of the effective M1 and GT operators as extracted from relevant experimental data for the sd shell nuclei using complete “ $0\hbar\omega$ ” wave functions. The immediate precursor to this series involved a similar analysis using wave functions based upon the Chung–Wildenthal interactions<sup>24,25)</sup>. The present series made use of wave functions based upon the new interaction of Wildenthal<sup>6)</sup> and includes an analysis of “mirror-level moments”<sup>1)</sup> and all Gamow-Teller beta decay<sup>4)</sup> together with the analysis of all magnetic moments and M1 gamma decay presented in this paper.

The magnetic moment and M1 gamma decay data that we considered here are remarkably well reproduced with the present wave functions together with a relatively simple parameterization of the effective  $g$ -factors. Furthermore, the values of the parameters which we extract are in overall good accord with the theoretical expectations based upon the calculated corrections which include the effects of higher-order configuration mixing and mesonic-exchange currents. The effect of mesonic-exchange currents shows up most clearly in the difference between the values of



the  $\delta_s$  parameters for the GT and the isovector M1 operators. Of all of the parameters, the  $\delta_p$  term for the isovector M1 operator is the most poorly accounted for by the calculations of refs. <sup>2,3</sup>). We propose that the "quenching" observed for the Gamow-Teller operator comes about approximately  $\frac{2}{3}$  from higher-order configuration mixing and  $\frac{1}{3}$  from  $\Delta$ -admixture.

We thank Dr. I. S. Towner for his many helpful comments on this work. This research was supported in part by the National Science Foundation under Grants No. PHY-86-11210 and PHY-85-09736.

### References

- 1) B.A. Brown and B.H. Wildenthal, *Phys. Rev.* **C28** (1983) 2397
- 2) I.S. Towner and F.C. Khanna, *Nucl. Phys.* **A399** (1983) 334
- 3) A. Arima, K. Shimizu, W. Bentz and H. Hyuga, *Adv. in Nucl. Phys.* to be published
- 4) B.A. Brown and B.H. Wildenthal, *At. Data Nucl. Data Tables* **33** (1985) 347
- 5) C.D. Goodman and S.D. Bloom, in *Spin excitations in nuclei*, ed F. Petrovich, G.E. Brown, G.T. Garvey, C.D. Goodman, R.A. Lindgren and W.G. Love (Plenum, New York, 1984) p. 143
- 6) B.H. Wildenthal, *Prog. Part. Nucl. Phys.* **11** (1984) 5
- 7) J.B. McGrory, *Phys. Lett.* **33B** (1970) 327
- 8) P.J. Brussaard and P.W. Glaudemans, *Shell-model applications in nuclear spectroscopy* (North-Holland, Amsterdam, 1977)
- 9) B.H. Wildenthal and B.A. Brown, unpublished.
- 10) A.R. Edmonds, *Angular momentum in quantum mechanics* (Princeton Univ. Press, 1960).
- 11) A. Arima, T. Cheon, K. Shimizu, H. Hyuga and T. Suzuki, *Phys. Lett.* **122B** (1983) 126
- 12) E. Oset and M. Rho, *Phys. Rev. Lett.* **42** (1979) 47
- 13) C.M. Lederer and V.S. Shirley, *Table of isotopes* (Wiley, New York, 1978)
- 14) M.C. Etchegoyen, A. Etchegoyen, B.H. Wildenthal, B.A. Brown and J. Keinonen, to be published
- 15) W.F. Rogers, D.L. Clark, S.B. Dutta, and A.G. Martin, *Phys. Lett.* **177B** (1986) 293
- 16) E.C. Adelberger, J.L. Osborne, H.E. Swanson and B.A. Brown, *Nucl. Phys.* **A417** (1984) 269
- 17) N. Anataraman, B.A. Brown, G.M. Crawley, A. Galonsky, A. Djalali, N. Marty, M. Morley, A. Willis, J.C. Jourdain and B.H. Wildenthal, *Phys. Rev. Lett.* **52** (1984) 1409
- 18) H. Sagawa, T.S.H. Lee and K. Ohta, *Phys. Rev.* **C33** (1986) 629
- 19) B. Serot and J.D. Walecka, *Adv. in Nucl. Phys.* **16** (1986) 1
- 20) A. Bouyssy, S. Marcos and J.F. Mathiot, *Nucl. Phys.* **A415** (1984) 497
- 21) H. Kurasawa and T. Suzuki, *Phys. Lett.* **165B** (1985) 234; *Nucl. Phys.* **A454** (1986) 527
- 22) J.A. McNeil *et al.*, *Phys. Rev.* **C34** (1986) 746
- 23) J. Delorme and I.S. Towner to be published in *Nucl. Phys. A.*
- 24) B.A. Brown, W. Chung and B.H. Wildenthal, *Phys. Rev. Lett.* **40** (1978) 1631
- 25) B.H. Wildenthal and W. Chung, *Mesons in nuclei*, vol. II, ed. M. Rho and D.H. Wilkinson, (North-Holland, Amsterdam, 1979), p. 751